Proc. Indian Acad. Sci. (Earth Planet. Sci.), Vol. 103, No. 1, March 1994, pp. 27–36.
© Printed in India.

Effects of transient uplift/erosion on the surface heat flow and heat generation relationship in presence of small scale asthenospheric convection

D V RAMANA and R N SINGH
National Geophysical Research Institute, Hyderabad 500007

MS received 5 June 1992; revised 14 February 1994

Abstract. In this paper the effect of transient uplift/erosion on the relationship between surface heat flow and heat generation for truncated exponential model of radiogenic heat source distribution and basal asthenospheric convection is investigated. Asthenospheric convection is described by a parameterized model, in the form of a nonlinear heat flux boundary condition involving basal temperature and mantle internal temperature. This boundary condition has been linearized and the analytical solution of the problem is obtained by the eigenvalue-eigenfunction expansion method. The analytical solution is used to derive the nature of surface heat flow and heat generation relationship. The results show that the linear relationship is maintained during the uplift/erosion and the estimates of the slope of the linear relationship are different from the depth scale of the exponential model and increase with the rate of uplift/erosion. The estimates of the reduced heat flow also increase with the rate of uplift/erosion. These results would find applications in the interpretation of linear surface heat flow and heat generation relationship which is observed in different tectonic environment.

Keywords. Uplift/erosion; truncated exponential model; parameterized convection; eigenvalue-eigenfunction; heat flow/heat generation.

1. Introduction

The heat flow and heat generation relationship has been interpreted using thermal models of the crust/lithosphere to derive the characteristics of the depth distribution of radioactive heat generation in the Earth. Birch *et al* (1968) and Roy *et al* (1968) in their pioneering studies proposed a step model of crustal radioactivity with the slope of the linear surface heat flow and heat generation relationship giving the thickness of uniform radiogenic heat layer. Lachenbruch (1970) subsequently proposed an exponential model of radioactive heat generation with the slope being equal to the logarithmic decrement of the model. He further showed that this model can better account for the differential erosion to which the geothermal provinces have invariably undergone. It has been also shown later that exponential model would also yield the linear relationship in presence of uplift and erosion but the slope would no longer be equal to the logarithmic decrement (Woodhouse and Birch 1980; Clark 1980 and Singh and Negi 1980). In these transient thermal model calculations the basal boundary conditions have been prescribed as constant heat flow at a greater depth. We would like to extend these studies by considering a boundary condition at the base of the lithosphere which characterizes ongoing small scale convection in the asthenosphere. The models of mantle convection below asthenosphere-lithosphere

interface can be used in specifying the basal boundary condition. The effect of boundary condition on the nature of the linear relationship has been obtained by extending lithosphere model by Lachenbruch and Sass (1978).

Sharpe and Peltier (1978) considered a parameterized model of mantle convection involving the relationship between Nusselt number and Rayleigh number to describe the thermal history of the earth. Richter (1984, 1985) has used the same procedure to determine the thermal state of the lithosphere. He obtained the following equation between heat flow and temperature at the top of the mantle:

$$F_r = K\frac{dT}{dZ} = \frac{1}{\pi^{1/2}}\left[\frac{g\alpha K^3}{kv}\right]^{1/3}(T_i - T)^{4/3}, \tag{1}$$

where F_r is the heat flux at the top mantle and g, α, K, k, and v are gravity, coefficient of thermal expansion, thermal conductivity, thermal diffusivity and viscosity of the asthenospheric material and T_i is the internal mantle temperature. This relation is non-linear. The equation (1) is approximated as

$$F_r = a - bT. \tag{2}$$

where

$$a = \frac{1}{\pi^{1/2}}\left[\frac{g\alpha K^3}{kv}\right]^{1/3}(T_i)^{4/3},$$

$$b = \frac{4a}{3T_i}.$$

We have retained only first order term as higher order terms are smaller compared to the first order term; ratio between first order and second order term is $\sim 0{\cdot}12$ for instance. For the distribution of the radiogenic heat with depth we consider the truncated exponential model by Costain and Decker (1987). Here the radiogenic heat decreases exponentially with depth from surface and the distribution is truncated at the base of the crust (figure 1). In this paper we obtain the thermal model using the boundary condition as equation (2) and use it to infer the nature of relationship between surface heat flow and heat generation.

2. Thermal model

The thermal model is constructed using the heat conduction theory for moving media. Temperature T in the lithosphere undergoing transient uplift/erosion is given by

$$\rho C\left[\frac{\partial T}{\partial t} - V\frac{\partial T}{\partial Z}\right] = K\left[\frac{\partial^2 T}{\partial Z^2}\right] + A(Z,t). \tag{3}$$

Here Z, t, ρ, C, V, K, $A(Z,t)$ are respectively depth coordinate, time, density, heat capacity, velocity of uplift and erosion, thermal conductivity and the rate of the radiogenic heat source. $A(Z,t)$ for truncated exponential model in presence of transient uplift/erosion is given by

$$A(Z,t) = A_0\exp(-(Z + Vt)/D)[H(Z) - H(Z - (L_c - Vt))]. \tag{4}$$

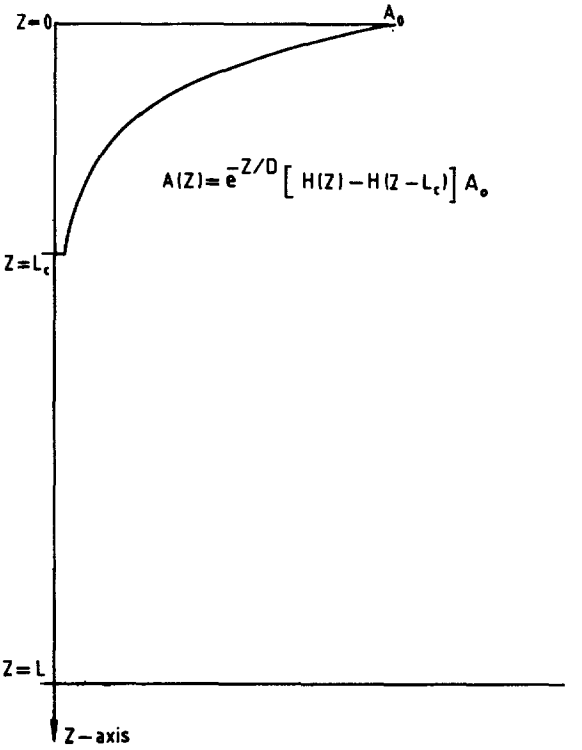

Figure 1. Geometric representation of the truncated exponential model of crustal radioactivity. A_0 and D are the initial surface heat generation and logarithmic decrement.

Here A_0 and L_c are the initial surface heat generation and the crustal thickness respectively.

The boundary conditions are:

$$T = 0 \qquad \text{at } Z = 0. \tag{5}$$

$$K\frac{dT}{dZ} = (a - bT) \quad \text{at } Z = L. \tag{6}$$

The initial condition is obtained by solving the steady state of equation (3) with $V = 0$ and the boundary conditions as equations (5) and (6). This implies that the small scale convection below lithosphere is going on before the start of uplift/erosion.

The solution of equation (3) with given boundary and initial conditions has been obtained by well-known eigenvalue-eigenfunction technique. The results are given as:

$$T(X,\tau) = NX + \sum_{n=0}^{\infty} \psi_n(\tau) B_n \sin(\lambda_n X) \exp(-(\mathrm{Pe}\, X/2 + \mathrm{Pe}^2 \tau/4)). \tag{7}$$

The expressions for all the terms appearing in equation (7) are given in Appendix 1.

The expression for surface heat flow $Q_s = K\,dT/dZ$ at $Z = 0$ is given as

$$Q_s = \frac{K}{L}\left[N + \sum_{n=0}^{\infty} \psi_n(\tau)\lambda_n B_n \exp(-\mathrm{Pe}^2\tau/4) \right]. \tag{8}$$

and the expression for surface heat generation is

$$A(t) = A_0 \exp(-Vt/D). \tag{9}$$

Equations (8) and (9) are used to obtain the linear heat flow and heat generation relationship.

3. Numerical results and discussions

The numerical results have been computed for surface heat flow (equation (8)) and surface heat generation (equation (9)). Figures 2 to 4 show the evolution of surface heat flow and heat generation for different values of initial surface heat generation $A_0 = 6{\cdot}27$, 4 and $2\,\mu\mathrm{W/m^3}$ with three different rates of uplift and erosion as $V = 100$, 300 and 500 m/Ma. The symbols on the curves of figures 2, 3 and 4 are spaced at 10 Ma intervals. In these computations we have taken $L = 100$ km, $L_c = 35$ km, $D = 10$ km, $K = 2{\cdot}5$ W/m°C, $k = 10^{-6}\,\mathrm{m^2/s}$, and $T_c = 1350$°C. The surface heat flow increases initially at the onset of uplift/erosion for some time and then starts decreasing

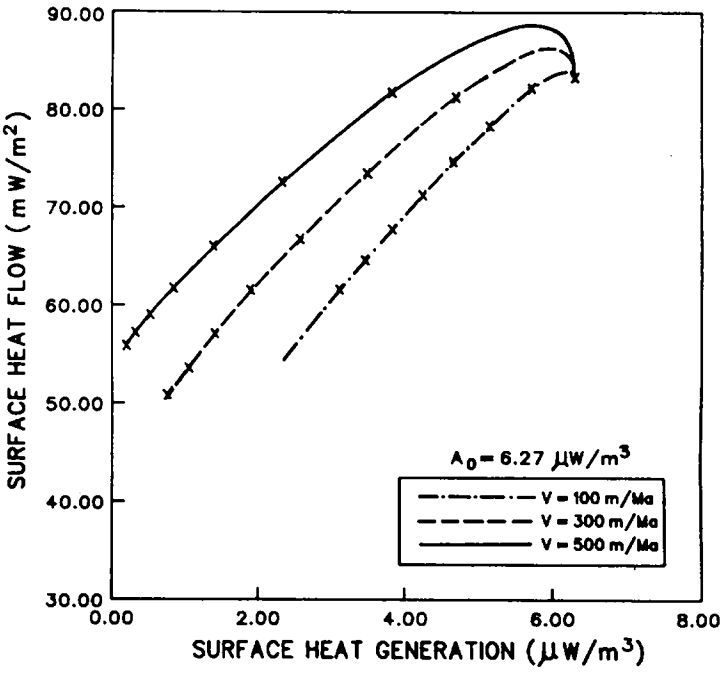

Figure 2. The evolution of the surface heat flow and heat generation with three different rates of uplift/erosion and with the initial surface heat generation $A_0 = 6{\cdot}27\,\mu\mathrm{W/m^3}$. Symbols on the curve are spaced at 10 Ma intervals.

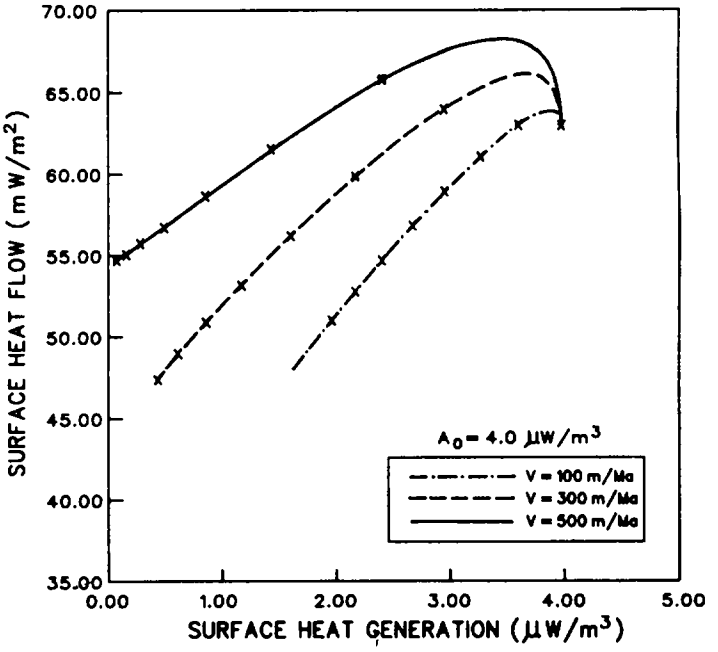

Figure 3. The evolution of the surface heat flow and heat generation with three different rates of uplift/erosion and with the initial surface heat generation $A_0 = 4{\cdot}00\,\mu W/m^3$. Symbols on the curve are spaced at 10 Ma intervals.

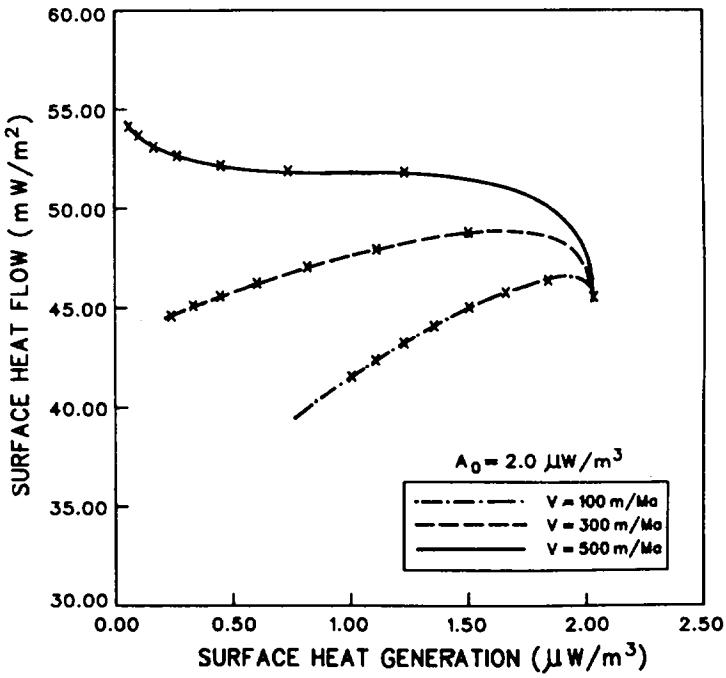

Figure 4. The evolution of the surface heat flow and heat generation with three different rates of uplift/erosion and with the initial surface heat generation $A_0 = 2{\cdot}00\,\mu W/m^3$. Symbols on the curve are spaced at 10 Ma intervals.

with time. The increase of surface heat flow is greater for high rate of uplift/erosion. This behaviour can be seen more significantly in figure 4 where the rate of uplift/erosion is 500 m/Ma and the initial surface heat generation 2·0 $\mu W/m^3$.

We construct the surface heat flow and heat generation relationship by following the approach of Woodhouse and Birch (1980) using one-dimensional calculations shown in figures 2, 3 and 4. This approach ignores the lateral heat transport effect. Here we assume that the surface values of radiogenic heat are different at different regions but the depth scale is same everywhere. We take three values of surface heat generation 2·0, 4·0 and 6·27 $\mu W/m^3$ and the depth scale as 10 km. The whole region is uplifted and eroded by the same rate. To calculate the heat flow at different times since the uplift/erosion, above one-dimensional calculations (figures 2, 3 and 4) are used. The relationship between surface heat flow and heat generation with the rate of uplift/erosion $V = 200$ m/Ma for different times are shown in figure 5. The relations are as: for $t = 0$ Ma, $Q_s = 27{\cdot}9 + 8{\cdot}8 \times 10^3 \times A_0$ and for $t = 20$ Ma, $Q_s = 33{\cdot}0 + 10{\cdot}1 \times 10^3 \times A_0$. We find that the relation between surface heat flow and heat generation remains linear during uplift/erosion. It is also observed that both the reduced heat flow and slope are increasing with time for the assumed values of L, D and V. Figure 6 shows the relations between surface heat flow and heat generation for different values of uplift/erosion, V, at time $t = 20$ Ma.

Tables 1, 2, 3 and 4 show the estimates of the reduced heat flow and slope at several times since the onset of uplift/erosion for different values of V, D, L and T_i which are obtained by following the above approach. From table 1, it is seen that the uplift/erosion rates significantly affect the estimates of the reduced heat flow and

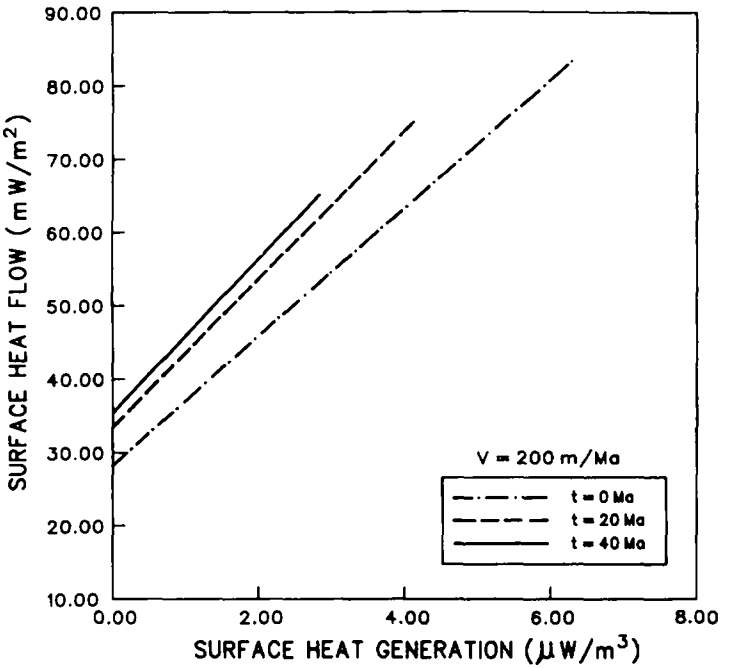

Figure 5. The relation between surface heat flow and heat generation at three different times of onset of uplift/erosion with $V = 200$ m/Ma ($t = 0$, 20 and 40 Ma).

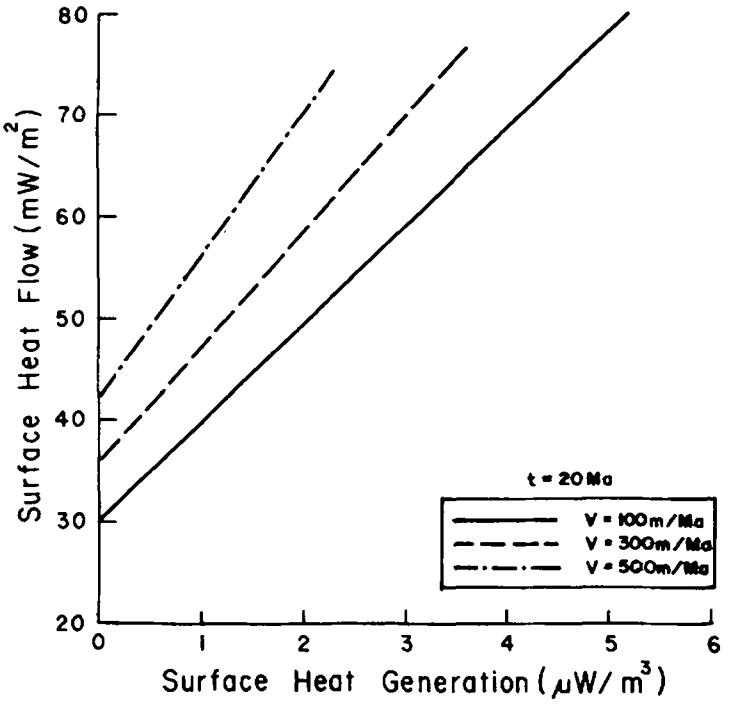

Figure 6. The relations between surface heat flow and heat generation at time 20 Ma with different values of rates of uplift/erosion ($V = 100$, 300 and 500 m/Ma).

Table 1. Reduced heat flow, Q_r, (mW/m^2) and slope, b, (km) for different values of rates of uplift/erosion with $T_i = 1350$°C, $L = 100$ km and $D = 10$ km.

Time	$V = 100$ m/Ma (Q_r, b)	$V = 300$ m/Ma (Q_r, b)	$V = 500$ m/Ma (Q_r, b)
0 Ma	(27·9, 8·8)	(27·9, 8·8)	(27·9, 8·8)
20 Ma	(30·4, 9·4)	(35·9, 11·4)	(42·2, 13·9)
40 Ma	(31·3, 9·6)	(39·2, 11·8)	(48·4, 15·7)

Table 2. Reduced heat flow, Q_r, (mW/m^2) and the slope, b, (km) for different values of logarithmic decrement with $T_i = 1350$°C, $L = 100$ km and $V = 200$ m/Ma.

Time	$D = 10$ km (Q_r, b)	$D = 15$ km (Q_r, b)	$D = 20$ km (Q_r, b)
0 Ma	(27·9, 8·8)	(27·9, 12·1)	(27·8, 14·5)
20 Ma	(33·0, 10·1)	(33·0, 13·6)	(33·0, 16·1)
40 Ma	(35·1, 10·5)	(35·1, 13·7)	(35·1, 16·1)

Table 3. Values of reduced heat flow, Q_r (mW/m^2) and slope, b (km) for different values of lithospheric thickness with $T_i = 1350°C$, $D = 10$ km and $V = 200$ m/Ma.

Time	$L = 100$ km (Q_r, b)	$L = 125$ km (Q_r, b)	$L = 150$ km (Q_r, b)
0 Ma	(27·9, 8·8)	(22·7, 8·9)	(19·1, 9·0)
20 Ma	(33.0, 10·1)	(26·9, 10·3)	(22·6, 10·5)
40 Ma	(35·1, 10·5)	(28·7, 10·9)	(24·3, 11·2)

Table 4. Values of reduced heat flow, Q_r (mW/m^2) and slope, b (km) for different values of internal mantle temperature, with $D = 10$ km, $L = 100$ km and $V = 200$ m/Ma.

Time	$T_i = 1350°C$ (Q_r, b)	$T_i = 1500°C$ (Q_r, b)	$T_i = 1750°C$ (Q_r, b)
0 Ma	(27·9, 8·8)	(31·0, 8·8)	(36·3. 8·8)
20 Ma	(33·0, 10·1)	(36·8, 10·1)	(43·1, 10·1)
40 Ma	(35·1, 10·5)	(39·1, 10·5)	(45·8, 10·5)

the slope. For uplift/erosion rate as 100 m/Ma we get the value of reduced heat flow as 30·4 mW/m^2 at 20 Ma whereas for uplift/erosion rate 500 m/Ma, the reduced heat flow increases to 42·1 mW/m^2. Similarly at 20 Ma the slope changes from 9·4 km for $V = 100$ m/Ma to 13·2 km for $V = 500$ m/Ma. Examination of tables 2, 3 and 4 show that changes in D does not affect the estimate of the reduced heat flow whereas changes in lithosphere thickness and mantle internal temperature does not change the estimate of slope. Thus the observed slope and reduced heat flow values should be corrected for uplift/erosion, as shown here, to obtain the exact value of the depth scale of crustal radioactivity and mantle heat flow for estimating the thermal state of the crust/lithosphere.

We wish to point out that the linear relationship after a long time since the cessation of uplift/erosion activity will return to the original line at $t = 0$. Thus asymptotic state would have no memory of the uplift/erosion to which the crust has been subjected. However, the thermal state will be different as the rate of heat generation has reduced.

4. Concluding remarks

We have presented an analytical thermal model of the lithosphere having basal asthenospheric small scale convection and undergoing transient uplift/erosion for a truncated exponential model of radiogenic heat. We have used this model to infer the linear heat flow and heat generation relationship. We have shown that the reduced heat flow and slope estimates vary with the rate of uplift/erosion, lithosphere thickness and with mantle internal temperature. These results can be used to estimate crustal radioactivity and also to understand the thermal tectonophysical problems such as metamorphism.

Appendix – 1

Expressions for the terms appearing in equation (7):

$$X = Z/L$$
$$\tau = (k/L^2)t$$
$$\mathrm{Pe} = VL/k$$
$$N = aL/(K + bL)$$

λ_n's are the eigenvalues which are the roots of the transidental equation

$$\lambda_n \cot(\lambda_n) + (M - \mathrm{Pe}/2) = 0$$

where

$$M = bL/K$$
$$B_n = (2)^{1/2}/[1 - (\sin(2\lambda_n))/(2\lambda_n)]^{1/2}$$
$$\psi_n(\tau) = \psi_n(0)\alpha(\tau) + A_1[n(\tau)b(-\tau) - n\alpha(\tau)] - B_1[m(\tau)b(-\tau) - m\alpha(\tau)] + f[c(\tau) - \alpha(\tau)] + g[b(+\tau) - \alpha(\tau)]$$

where

$$\psi_n(0) = B_n\{Ad^2[Q - P] + [M_1 - N]R + [M_2 - N]S + N_2 T_1\}$$
$$A = A_0 L^2/K$$
$$d = D/L$$
$$Q = [\exp(\mathrm{Pe}\,\beta/2)((\mathrm{Pe}/2)\sin(\lambda_n\beta) - \lambda_n\cos(\lambda_n\beta)) + \lambda_n]/D_n$$
$$P = [\exp(C_1\beta)(C_1\sin(\lambda_n\beta) - \lambda_n\cos(\lambda_n\beta)) + \lambda_n]/C_n$$
$$M_1 = M_2 - Ad\beta\exp(-\beta/d)$$
$$R = [\exp(\mathrm{Pe}\,\beta/2)((\mathrm{Pe}\,\beta/2 - E_n/D_n)\sin(\lambda_n\beta) - (\lambda_n\beta - \lambda_n\mathrm{Pe}/D_n)\cos(\lambda_n\beta)) - \lambda_n\mathrm{Pe}/D_n]/D_n$$
$$M_2 = (aL - bLN_2)/(K + bL) - Ad\exp(-\beta/d)$$
$$S = \{\exp(\mathrm{Pe}/2)[(\mathrm{Pe}/2)\sin(\lambda_n) - \lambda_n\cos(\lambda_n)] - \exp(\mathrm{Pe}\,\beta/2)[(\mathrm{Pe}\,\beta/2)\sin(\lambda_n\beta) - \lambda_n\cos(\lambda_n\beta)]\}/D_n$$
$$N_2 = Ad^2[1 - \exp(-\beta/d)] - Ad\beta\exp(-\beta/d)$$
$$T_1 = \{\exp(\mathrm{Pe}/2)[(\mathrm{Pe}/2 - E_n/D_n)\sin(\lambda_n) - (\lambda_n - \lambda_n\mathrm{Pe}/D_n)\cos(\lambda_n)] - \exp(\mathrm{Pe}\,\beta/2)[(\mathrm{Pe}\,\beta/2 - E_n/D_n)\sin(\lambda_n\beta) - (\lambda_n\beta - \lambda_n\mathrm{Pe}/D_n)\cos(\lambda_n\beta)]\}/D_n$$
$$\beta = L_c/L$$
$$D_n = (\mathrm{Pe}/2)^2 + \lambda_n^2$$
$$C_1 = \mathrm{Pe}/2 - 1/d$$
$$C_n = (\mathrm{Pe}/2 - 1/d)^2 + \lambda_n^2$$
$$E_n = (\mathrm{Pe}^2/4 - \lambda_n^2)$$
$$\alpha(\tau) = \exp(-\lambda_n^2\tau)$$
$$A_1 = B_n A C_1 \exp(C_1\beta)/C_n$$
$$n(\tau) = [-E_n\sin(C_t) + \lambda_n\mathrm{Pe}\cos(C_t)]/Q_n$$
$$b(\pm\tau) = \exp(\pm\,\mathrm{Pe}^2\tau/4)$$
$$n = [-E_n\sin(\lambda_n) + \lambda_n\mathrm{Pe}\cos(\lambda_n)]/Q_n$$
$$B_1 = B_n A\lambda_n\exp(C_1\beta)/C_n$$
$$m(\tau) = [-E_n\cos(C_t) - \lambda_n\mathrm{Pe}\sin(C_t)]/Q_n$$
$$m = [-E_n\cos(\lambda_n) - \lambda_n\mathrm{Pe}\sin(\lambda_n)]/Q_n$$
$$f = B_n A\lambda_n/G_n$$
$$c(\tau) = \exp((\mathrm{Pe}^2/4 - \mathrm{Pe}/d)\tau)$$
$$g = B_n\mathrm{Pe}\,NQ_1/D_n$$

$$C_t = \lambda_n(\beta - \mathrm{Pe}\,\tau)$$
$$Q_n = (\lambda_n^2 - \mathrm{Pe}^2/4)^2 + (\lambda_n \mathrm{Pe})^2$$
$$G_n = (\mathrm{Pe}^2/4 - \mathrm{Pe}/d) + \lambda_n^2$$
$$Q_1 = \{\exp(\mathrm{Pe}/2)[(\mathrm{Pe}/2)\sin(\lambda_n) - \lambda_n \cos(\lambda_n)] - \lambda_n\}/D_n$$

Acknowledgement

Authors are grateful to Director, National Geophysical Research Institute, Hyderabad for his kind encouragement and permission to publish this work.

References

Birch F, Roy R F and Decker E R 1968 Heat flow and thermal history in New England and New York; In: *Studies of Appalachian Geology* (ed) E An-Ze (New York: Interscience) pp. 437–451

Clark S P 1980 Comments on paper by T C Lee on 'erosion, uplift, exponential heat source distribution and transient heat flux'; *J. Geophys. Res.* **85** 2694–2695

Costain J K and Decker E R 1987 Heat flow at the proposed Appalachian ultradeep corehole (ADCOH) site, Tectonic implications; *Geophys. Res. Lett.* **14** 252–255

Lachenbruch A H 1970 Crustal temperature and heat production: Implication of the linear heat flow relation; *J. Geophys. Res.* **75** 3291–3300

Lachenbruch A H and Sass J H 1978 Models of an extending lithosphere and heat flow in the basin and range province; *Geol. Soc. Am. Mem.* **152** 209–250

Richter F M 1984 Regionalised models for the thermal evolution of the Earth; *Earth Planet. Sci. Lett.* **68** 471–484

Richter F M 1985 Models for the Archean thermal regime; *Earth Planet. Sci. Lett.* **73** 350–360

Roy R F, Blackwell D D and Birch F 1968 Heat generation in plutonic rocks and continental heat flow provinces; *Earth Planet. Sci. Lett.* **5** 1–12

Singh R N and Negi J G 1980 Comments on paper by T C Lee on erosion, uplift, exponential heat source distribution and transient heat flux'; *J. Geophys. Res.* **85** 2696–2697

Sharpe H N and Peltier W R 1978 Parameterized convection and the earth's thermal history; *Geophys. Res. Lett.* **5** 737–740

Woodhouse J H and Birch F 1980 Comments on paper by T C Lee on 'erosion, uplift, exponential heat source distribution and transient heat flux'; *J. Geophys. Res.* **85** 2693–2694